CLEO CONF 96-18
ICHEP96 PA05-73

# Search for $b \to s$ gluon via Inclusive $B \to \eta^{'}$ and $B \to K_s$ Decays.

CLEO Collaboration

(July 22, 1996)

## Abstract

Using a data sample with an integrated luminosity of 3 $\mathrm{fb}^{-1}$, we report the first observation of inclusive $B \to \eta^{'}$ transitions. We have measured the branching fraction and the momentum spectrum of these transitions which arise from $b \to c$ processes and find $\mathcal{B}(B \to \eta^{'} X) = (3.06 \pm 0.61(stat) \pm 0.55(sys)) \times 10^{-2}$ for 0.5 GeV/$c$ $< p_{\eta^{'}} <$ 2.0 GeV/$c$ We have also searched for evidence of $b \to s$ gluon processes which give rise to $\eta^{'}$ or $K_s$ mesons with momenta in the range 2.0 GeV/$c$ $< p <$ 2.7 GeV/$c$ where there is little background from $b \to c$ processes.

M. Artuso,[1] A. Efimov,[1] M. Gao,[1] M. Goldberg,[1] R. Greene,[1] F. Frasconi,[1] D. He,[1] S. Kopp,[1] G. C. Moneti,[1] R. Mountain,[1] Y. Mukhin,[1] S. Schuh,[1] T. Skwarnicki,[1] S. Stone,[1] X. Xing,[1] J. Bartelt,[2] S. E. Csorna,[2] V. Jain,[2] S. Marka,[2] A. Freyberger,[3] R. Godang,[3] D. Gibaut,[3] K. Kinoshita,[3] I. C. Lai,[3] P. Pomianowski,[3] S. Schrenk,[3] G. Bonvicini,[4] D. Cinabro,[4] L. Perera,[4] B. Barish,[5] M. Chadha,[5] S. Chan,[5] G. Eigen,[5] J. S. Miller,[5] C. O'Grady,[5] M. Schmidtler,[5] J. Urheim,[5] A. J. Weinstein,[5] F. Würthwein,[5] D. M. Asner,[6] D. W. Bliss,[6] W. S. Brower,[6] G. Masek,[6] H. P. Paar,[6] J. Gronberg,[7] C. M. Korte,[7] D. J. Lange,[7] R. Kutschke,[7] S. Menary,[7] R. J. Morrison,[7] S. Nakanishi,[7] H. N. Nelson,[7] T. K. Nelson,[7] C. Qiao,[7] J. D. Richman,[7] D. Roberts,[7] A. Ryd,[7] H. Tajima,[7] M. S. Witherell,[7] R. Balest,[8] B. H. Behrens,[8] K. Cho,[8] W. T. Ford,[8] H. Park,[8] P. Rankin,[8] J. Roy,[8] J. G. Smith,[8] J. P. Alexander,[9] C. Bebek,[9] B. E. Berger,[9] K. Berkelman,[9] K. Bloom,[9] D. G. Cassel,[9] H. A. Cho,[9] D. M. Coffman,[9] D. S. Crowcroft,[9] M. Dickson,[9] P. S. Drell,[9] R. Ehrlich,[9] R. Elia,[9] A. D. Foland,[9] P. Gaidarev,[9] B. Gittelman,[9] S. W. Gray,[9] D. L. Hartill,[9] B. K. Heltsley,[9] P. I. Hopman,[9] S. L. Jones,[9] J. Kandaswamy,[9] N. Katayama,[9] P. C. Kim,[9] D. L. Kreinick,[9] T. Lee,[9] Y. Liu,[9] G. S. Ludwig,[9] J. Masui,[9] J. Mevissen,[9] N. B. Mistry,[9] C. R. Ng,[9] E. Nordberg,[9] M. Ogg,[9,*] J. R. Patterson,[9] D. Peterson,[9] D. Riley,[9] A. Soffer,[9] C. Ward,[9] P. Avery,[10] M. Athanas,[10] C. D. Jones,[10] M. Lohner,[10] C. Prescott,[10] S. Yang,[10] J. Yelton,[10] J. Zheng,[10] G. Brandenburg,[11] R. A. Briere,[11] D. Y.-J. Kim,[11] T. Liu,[11] M. Saulnier,[11] R. Wilson,[11] H. Yamamoto,[11] T. E. Browder,[12] F. Li,[12] Y. Li,[12] J. L. Rodriguez,[12] T. Bergfeld,[13] B. I. Eisenstein,[13] J. Ernst,[13] G. E. Gladding,[13] G. D. Gollin,[13] E. Johnson,[13] I. Karliner,[13] M. Palmer,[13] M. Selen,[13] J. J. Thaler,[13] K. W. Edwards,[14] A. Bellerive,[15] D. I. Britton,[15] R. Janicek,[15] D. B. MacFarlane,[15] K. W. McLean,[15] P. M. Patel,[15] A. J. Sadoff,[16] R. Ammar,[17] P. Baringer,[17] A. Bean,[17] D. Besson,[17] D. Coppage,[17] C. Darling,[17] R. Davis,[17] N. Hancock,[17] S. Kotov,[17] I. Kravchenko,[17] N. Kwak,[17] S. Anderson,[18] Y. Kubota,[18] M. Lattery,[18] J. J. O'Neill,[18] S. Patton,[18] R. Poling,[18] T. Riehle,[18] A. Smith,[18] V. Savinov,[18] M. S. Alam,[19] S. B. Athar,[19] Z. Ling,[19] A. H. Mahmood,[19] H. Severini,[19] S. Timm,[19] F. Wappler,[19] A. Anastassov,[20] S. Blinov,[20,†] J. E. Duboscq,[20] R. Fulton,[20] D. Fujino,[20] K. K. Gan,[20] T. Hart,[20] K. Honscheid,[20] H. Kagan,[20] R. Kass,[20] J. Lee,[20] M. Sung,[20] A. Undrus,[20,†] R. Wanke,[20] A. Wolf,[20] M. M. Zoeller,[20] B. Nemati,[21] S. J. Richichi,[21] W. R. Ross,[21] P. Skubic,[21] M. Wood,[21] M. Bishai,[22] J. Fast,[22] E. Gerndt,[22] J. W. Hinson,[22] D. H. Miller,[22] E. I. Shibata,[22] I. P. J. Shipsey,[22] M. Yurko,[22] L. Gibbons,[23] S. D. Johnson,[23] Y. Kwon,[23] S. Roberts,[23] E. H. Thorndike,[23] C. P. Jessop,[24] K. Lingel,[24] H. Marsiske,[24] M. L. Perl,[24] S. F. Schaffner,[24] D. Ugolini,[24] R. Wang,[24] X. Zhou,[24] T. E. Coan,[25] V. Fadeyev,[25] I. Korolkov,[25] Y. Maravin,[25] I. Narsky,[25] V. Shelkov,[25] R. Stroynowski,[25] J. Staeck,[25] I. Volobouev,[25] and J. Ye[25]

[1]Syracuse University, Syracuse, New York 13244
[2]Vanderbilt University, Nashville, Tennessee 37235
[3]Virginia Polytechnic Institute and State University, Blacksburg, Virginia 24061

---

[*]Permanent address: University of Texas at Austin.

[†]Permanent address: BINP, RU-630090 Novosibirsk, Russia.

[4]Wayne State University, Detroit, Michigan 48202
[5]California Institute of Technology, Pasadena, California 91125
[6]University of California, San Diego, La Jolla, California 92093
[7]University of California, Santa Barbara, California 93106
[8]University of Colorado, Boulder, Colorado 80309-0390
[9]Cornell University, Ithaca, New York 14853
[10]University of Florida, Gainesville, Florida 32611
[11]Harvard University, Cambridge, Massachusetts 02138
[12]University of Hawaii at Manoa, Honolulu, Hawaii 96822
[13]University of Illinois, Champaign-Urbana, Illinois 61801
[14]Carleton University, Ottawa, Ontario, Canada K1S 5B6
and the Institute of Particle Physics, Canada
[15]McGill University, Montréal, Québec, Canada H3A 2T8
and the Institute of Particle Physics, Canada
[16]Ithaca College, Ithaca, New York 14850
[17]University of Kansas, Lawrence, Kansas 66045
[18]University of Minnesota, Minneapolis, Minnesota 55455
[19]State University of New York at Albany, Albany, New York 12222
[20]Ohio State University, Columbus, Ohio 43210
[21]University of Oklahoma, Norman, Oklahoma 73019
[22]Purdue University, West Lafayette, Indiana 47907
[23]University of Rochester, Rochester, New York 14627
[24]Stanford Linear Accelerator Center, Stanford University, Stanford, California 94309
[25]Southern Methodist University, Dallas, Texas 75275

# I. INTRODUCTION

In this paper we report a first measurement of $\mathcal{B}(B \to \eta' X)$ for $\eta'$ momenta below 2.0 GeV/$c$ and searches for $\eta'$ and $K_s$ mesons above the kinematic limit for $b \to c$ processes.

CLEO has previously reported measurements of $\mathcal{B}(B \to \eta X)$ [1]. In $B$ decay the largest sources of $\eta'$ mesons are the processes $B \to D_s X$ with $D_s \to \eta'$, $B \to D^0 X$ with $D^0 \to \eta'$, $B \to D^+ X$ with $D^+ \to \eta'$ and $B \to \Lambda_c X$ with $\Lambda_c \to \eta'$. According to the CLEO Monte Carlo simulation, these are expected to account for 36%, 28%, 4% and 2.1% of the $\eta'$ mesons from $B$ decay, respectively. Note that even though the $D^0 \to \eta'$, $D^+ \to \eta'$ and $\Lambda_c \to \eta'$ transitions are Cabibbo suppressed, due to the large values of $B \to D^0$, $B \to D^+$ and $B \to \Lambda_c$ branching fractions, these are appreciable sources of $\eta'$s. The other source is $s\bar{s}$ quark popping, which accounts for 26.5% of the $\eta'$ mesons. The momentum spectrum expected for $\eta'$ mesons from these sources is shown in Fig. 1.

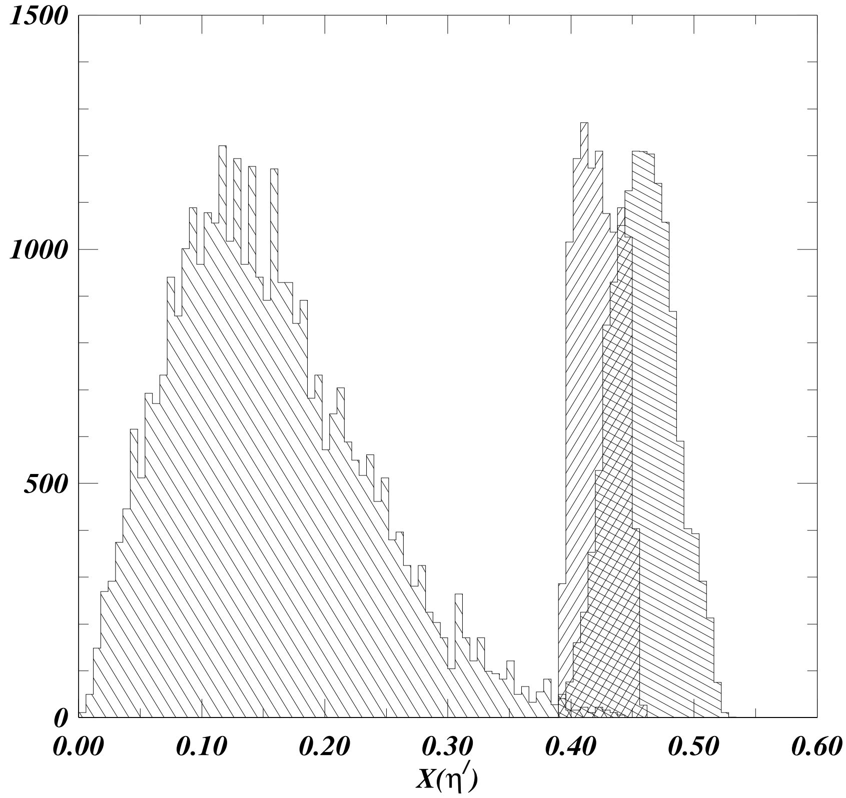


FIG. 1. The $x(\eta')$ (scaled momentum) distributions for the different physical mechanisms which produce $\eta'$s. The histogram (cross-hatched downwards at a steep angle) is a simulation of $\eta'$ production from generic $B$ decays. In the range $x(\eta') > 0.4$, the histogram (cross-hatched upwards) is $\eta'$ from $B \to D^{(*)}\eta'$ and the histogram (cross-hatched downwards) shows $\eta'$ from a MC simulation of $B \to \eta' K^{(*)}$, The normalization of these quasi two-body components is arbitrary.

A search for inclusive signatures of $b \to s$ gluon rather than exclusive signatures has two possible advantages. The inclusive rate may be calculable from first principles and is expected to be at least an order of magnitude larger than the rate for any exclusive channel. For example, the branching fraction for $b \to sq\bar{q}$ (where $q = u,\ d,\ s$) is $\mathcal{O}(1\%)$ [2], [3] and the branching fraction for the inclusive process $b \to s\bar{s}s$ is expected to be $\sim 0.23\%$ in the Standard Model [3], while low multiplicity decay modes such as $\bar{B}^0 \to \phi K_s$ or $\bar{B}^0 \to K^-\pi^+$ are expected to have branching fractions of order $10^{-5}$. The disadvantage of the inclusive method is the severe continuum background that must be subtracted or suppressed.

The decay $B \to \eta^{'} X_s$, where $X_s$ denotes a meson containing an $s$ quark, is dominated by the gluonic penguin, $b \to sg^* \to s\bar{s}s$. The decay $B \to K_s X$, where $X$ denotes a meson which contains no $s$ quark, arises from a similiar gluonic penguin, $b \to sg^* \to s\bar{d}d$. In both cases, the experimental signature of the gluonic penguin process considered in this paper is mesons which are too energetic to originate from $b \to c$ transitions.

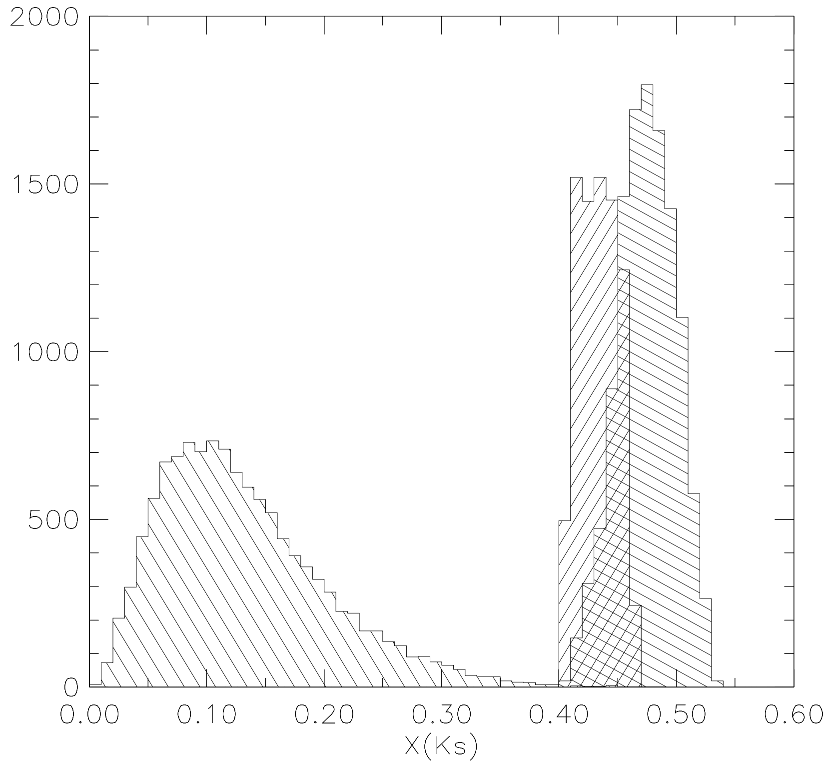


FIG. 2. The $x(K_s)$ (scaled momentum) distributions for the different physical mechanisms which produce $K_s$ mesons. The region $0.39 < x(K_s) < 0.54$ corresponds to $2.1 < p_{K_s} < 2.9$ GeV. The histogram (cross-hatched downwards) shows $K_s$ from a MC simulation of $b \to c$ decays. In the range $x(K_s) > 0.39$, the histogram (cross-hatched upwards) is $K_s$ from $B \to D^{(*)} K_s$ and the histogram (cross-hatched downwards at a small angle) is a simulation of $K_s$ production from quasi-two body modes such as $B \to K_s\pi$, $B \to K_s\rho$ $B \to K_s\rho^{(')}$ decays which are $b \to s\ g$ processes. The normalization of the quasi two-body component is arbitrary.

An analogous search for $b \to sg^*$, $g^* \to s\bar{s}$ was previously carried out by CLEO using high momentum $\phi$ production [6]. In the search for high momentum $\phi$ production, limits were obtained using two complementary techniques. A purely inclusive technique with shape cuts gave a limit $\mathcal{B}(B \to X_s\phi) < 2.2 \times 10^{-4}$ for $2.0 < p_\phi < 2.6$ GeV. Using the $B$ reconstruction technique, in which combinations of the $\phi$ candidate, a kaon, and up to 4 pions were required to be consistent with a $B$ candidate, gave a limit of $\mathcal{B}(B \to X_s\phi) < 1.1 \times 10^{-4}$ for $M_{X_s} < 2.0$ GeV, corresponding to $p_\phi > 2.1$ GeV. These results can be compared to the Standard Model calculation of Deshpande *et al.* [4], which predicts that the branching fraction for this process should lie in the range $(0.6 - 2.0) \times 10^{-4}$ and that 90% of the $\phi$ mesons from this mechanism will lie in the range of the experimental search. A similiar result was obtained by Ciuchini *et al.* [5] who predict a branching fraction for $\mathcal{B}(B \to X_s\phi)$ in the range $(1.1 \pm 0.9) \times 10^{-4}$. One sees that the sensitivity of the inclusive method is nearly sufficient to observe a signal from Standard Model $b \to s\ g$.

In the case of $\eta^{'}$, the signature of the gluonic penguin is reconstructed $\eta^{'}$ mesons with $2.0 < p_{\eta'} < 2.7$ GeV/c. A search in this kinematic range will avoid contamination from most $\eta^{'}$ mesons produced by $b \to c$ mechanisms, as is shown in Fig. 1. In the case of the $\eta^{'}$, internal spectator decays from the quark level $b \to c\bar{u}d$ process (i.e. $\bar{B}^0 \to D^{(*)0}\eta^{'}$) may also contribute to the high momentum signal region.

Similiarly, the principal sources of $K_s$ mesons in B decays are the processes $B \to D_s X$ with $D_s \to K_s$, $B \to D^0 X$ with $D^0 \to K_s$, $B \to D^+ X$ with $D^+ \to K_s$ and $B \to \Lambda_c X$ with $\Lambda_c \to K_s$. These sources produce $K_s$ mesons with momenta below 2.0 GeV/c. The decay $B \to K_s X$, where $X$ denotes a particle which does not contain an $s$ quark, is the signature of the gluonic penguin $b \to sg^* \to s\bar{d}d$. This mechanism will give rise to $K_s$ mesons with momenta above 2.0 GeV as shown in Fig. 2. In addition, $B \to K_s D^{(*)}$ from the Cabibbo suppressed internal spectator processes $b \to c\bar{u}s$ may contribute in this kinematic range.

## II. DATA SAMPLE AND SELECTION CRITERIA

The data sample used contains 3.111 fb$^{-1}$ of on-resonance data and 1.609 fb$^{-1}$ of below resonance data which is used for background subtraction. This sample contains $3.3 \times 10^6$ $B\bar{B}$ pairs. The scale factor for the subtraction, including the correction for the energy dependence of the continuum cross section, is $f = 1.91 \pm 0.01(sys)$.

The analysis is performed in terms of the scaled momentum of the meson

$$x = \frac{p_{meson}}{\sqrt{(E_{beam}^2 - m_{meson}^2)}}$$

to allow the continuum to be subtracted correctly. The bins above the signal region are used as a consistency check of the continuum background subtraction and the analysis procedure.

Shape cuts are used to suppress the continuum background in both inclusive analyses. We have combined three useful shape variables using a Fisher discriminant (also known as a multivariate linear discriminant). The variables used are $R_2$, $E_{20}$, $E_{40}$, defined below.

1. $R_2$: The ratio of the second and zeroth Fox-Wolfram moments. This variable is similiar to sphericity. Small values of $R_2$ correspond to spherical events, while values near one correspond to jetlike events.

2. $E_{20}$: The sum of the energies in $20^o$ cones around the $\eta^{'}$ direction, and around the direction opposite to the $\eta^{'}$. All tracks and unmatched showers are considered except those which form the $\eta^{'}$ candidate.

3. $E_{40}$: This quantity is computed in the same way as $E_{20}$ except the cone opening angles are $40^o$.

A Fisher discriminant combines several variables, which individually may only marginally separate signal from background, to create a single variable which has better signal to background discrimination. The Fisher discriminant is defined as:

$$F = \Sigma_{i=1}^{3} \alpha_i x_i,$$

where $\alpha_i$ is the coefficient for the $i$th shape variable $x_i$. The coefficients $\alpha_i$ are calculated to maximize the separation between signal and background.

The values of $\alpha_i$ were determined using samples of continuum and $B\bar{B}$ Monte Carlo events. The optimal cuts on the Fisher discriminants were also determined by maximizing $S^2/B$ for Monte Carlo samples.

## III. RESULTS ON $\eta'$ MESONS FROM $B \to C$ TRANSITIONS.

Pairs of oppositely charged track candidates consistent with originating from the origin are combined with $\eta \to \gamma\gamma$ candidates to form $\eta'$ candidates. Photon candidates with energies above 30 MeV are used to form the $\eta$ candidates. Photons which are consistent with having originated from a $\pi^0$ with momentum above 800 MeV are rejected. The $\eta$ candidates with invariant mass within $2.5\sigma$ of the $\eta$ mass are kinematically fitted to the nominal $\eta$ mass and then combined with two charged track candidates to form an $\eta'$ candidate.

Two approaches to fitting the data have been tried. It is possible either to fit the $\eta\pi^+\pi^-$ invariant mass plots in the on-resonance and off-resonance samples separately and then subtract the resulting yields, or to fit the continuum-subtracted $\eta\pi^+\pi^-$ invariant mass plots. The former method is chosen to obtain the final result. The fits to the on-resonance and below-resonance samples are shown in Figs. 3, 4, 5, 6, and 7. The yields as a function of $x$ are given in Table II. In order to improve the statistical power of the tests of the continuum subtraction, the cuts on the Fischer discriminant are loosened for bins above the signal region, which will henceforth be referred to as the "control bins". Efficiencies were determined from Monte Carlo simulation of $B\bar{B}$ decay for $x(\eta') < 0.52$. For the control bins, the efficiency was taken to be the same as for $B\bar{B}$ events with $0.45 < x(\eta') < 0.52$, but using the loosened cuts. The differential branching fraction as a function of $x$, and the expectations from the CLEO Monte Carlo simulation, are shown in Fig. 8. The results are in agreement.

The background shape is the largest component of the systematic error for the determination of the branching fraction in the low momentum region and in the $b \to s\ g$ search. It is determined by comparing fits with different background parameterizations. The continuum oversubtraction error, which is small in this analysis, is determined from parametric Monte Carlo studies and is discussed in detail in section IV B. The errors on the signal parameters are determined from the yield with the mean of the $\eta'$ signal fixed to the value from Monte Carlo simulation, which is shifted by 1 MeV with respect to the value found in data. There is also a contribution of 9% from the uncertainty in the detection efficiency. The components of the systematic uncertainty are listed in Table I.

The branching fractions from the bins in scaled momentum are summed together, after correcting for the x-dependent detection efficiency and the $\eta^{'} \rightarrow \eta\pi^{+}\pi^{-}$ and $\eta \rightarrow \gamma\gamma$ branching fractions. This gives

$$\mathcal{B}(B \rightarrow \eta^{'} X) = (3.06 \pm 0.61(stat) \pm 0.55(sys)) \times 10^{-2}$$

for $0.10 < x(\eta^{'}) < 0.39$. This can be compared to the prediction of the CLEO Monte Carlo simulation of 3.79%. The simulation is a compilation of measured exclusive branching fractions and uses a fragmentation model for unmeasured channels. This is the first observation of inclusive $B$ decays to $\eta^{'}$.

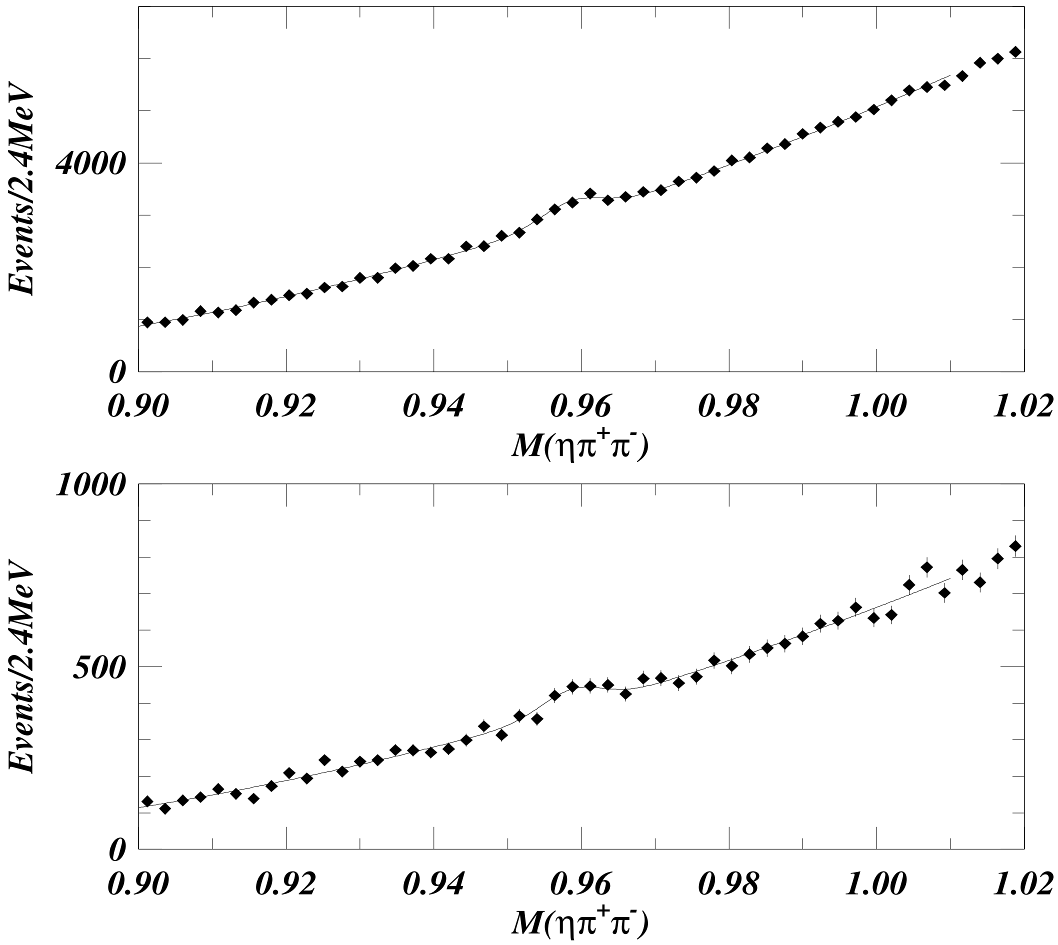


FIG. 3. The $\eta\pi^+\pi^-$ invariant mass distribution for $0.10 < x < 0.20$. The top plot is on-resonance data while the bottom plot is data taken below resonance.

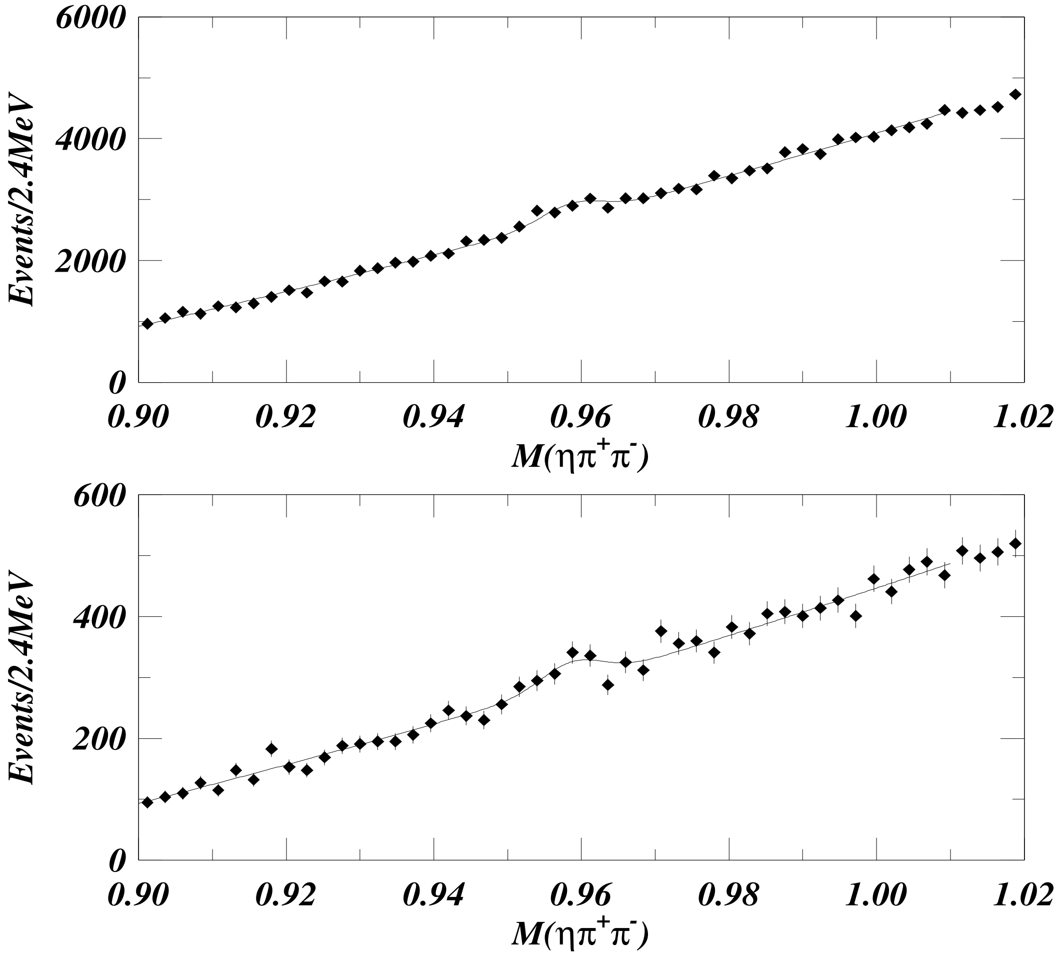


FIG. 4. The $\eta\pi^+\pi^-$ invariant mass distribution for $0.20 < x < 0.28$ The top plot is on-resonance data while the bottom plot is data taken below resonance.

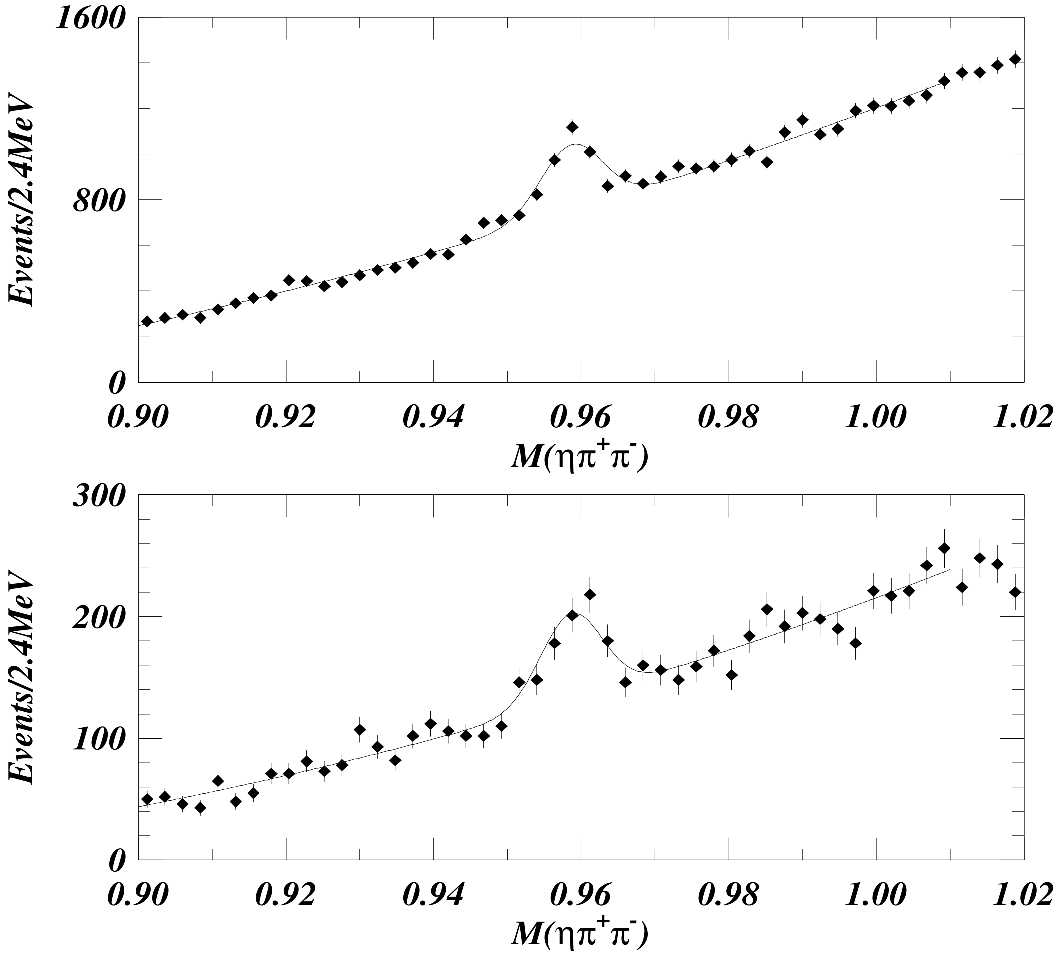


FIG. 5. The $\eta\pi^+\pi^-$ invariant mass distribution for $0.28 < x < 0.39$ The top plot is on-resonance data while the bottom plot is data taken below resonance.

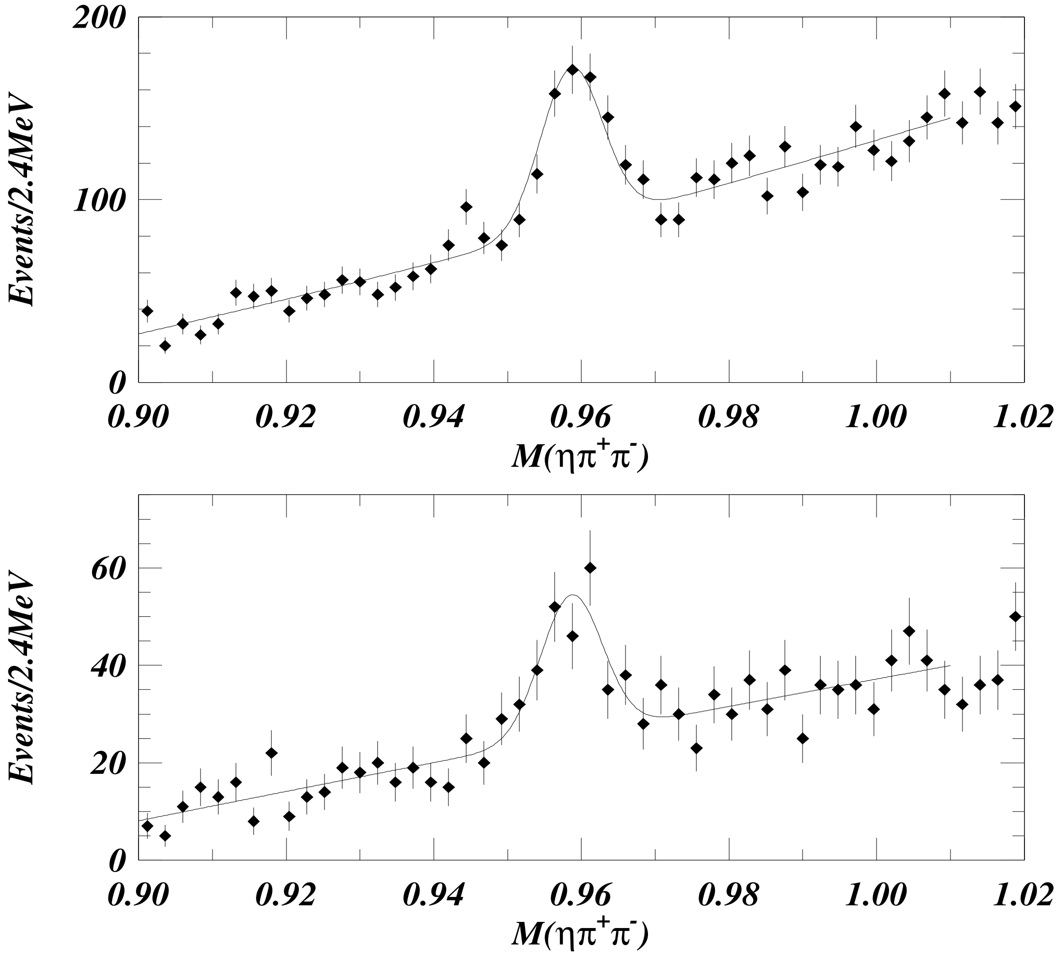


FIG. 6. The $\eta\pi^+\pi^-$ invariant mass distribution for $0.39 < x < 0.45$ The top plot is on-resonance data while the bottom plot is data taken below resonance.

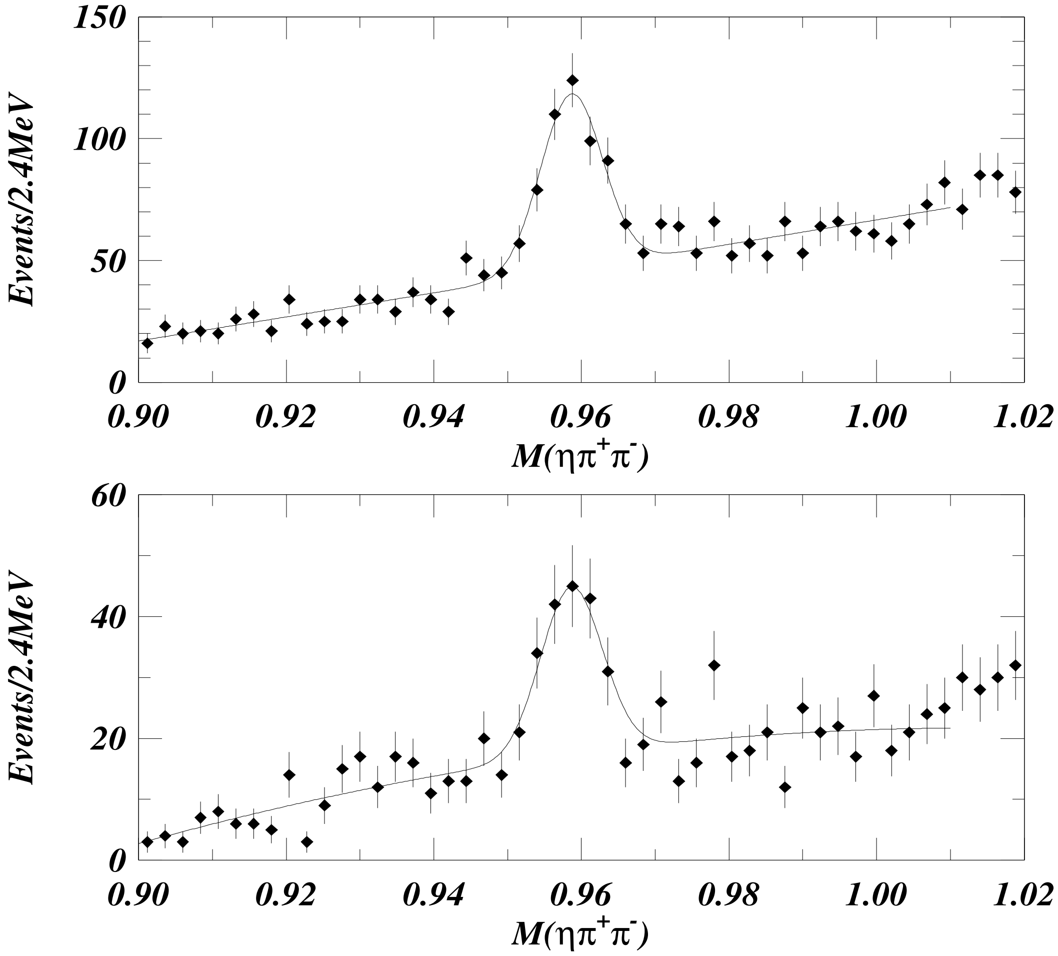


FIG. 7. The $\eta\pi^+\pi^-$ invariant mass distribution for $0.45 < x < 0.52$ The top plot is on-resonance data while the bottom plot is data taken below resonance.

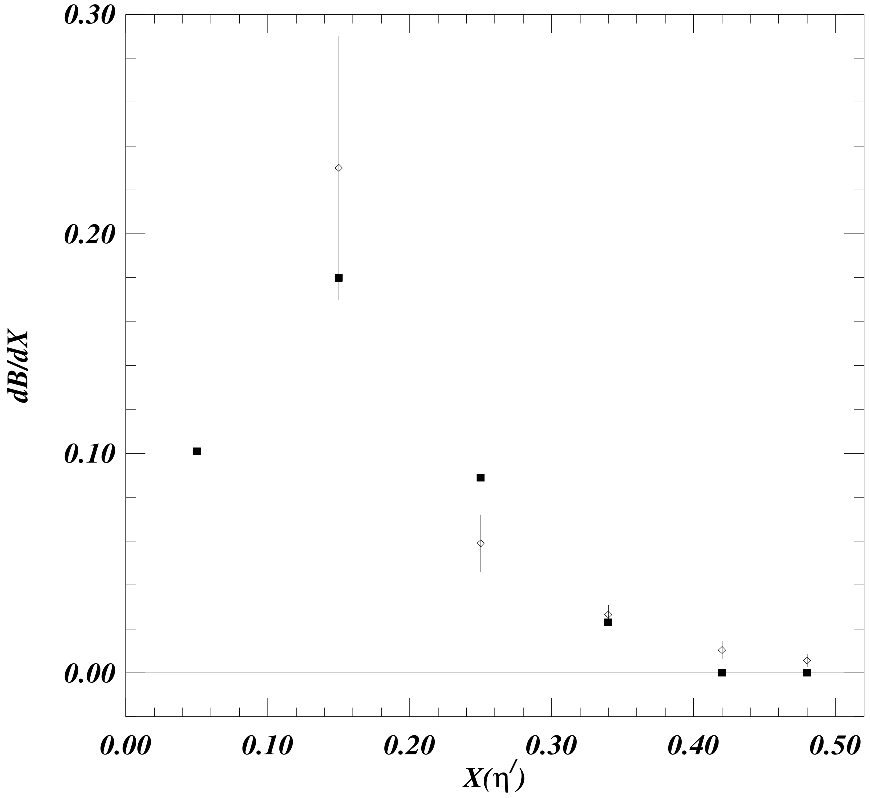


FIG. 8. The distribution of $d\mathcal{B}(B \to \eta^{'})/dx$ as a function of $x$ in data (open diamonds with error bars) compared to the CLEO Monte Carlo simulation (filled squares).

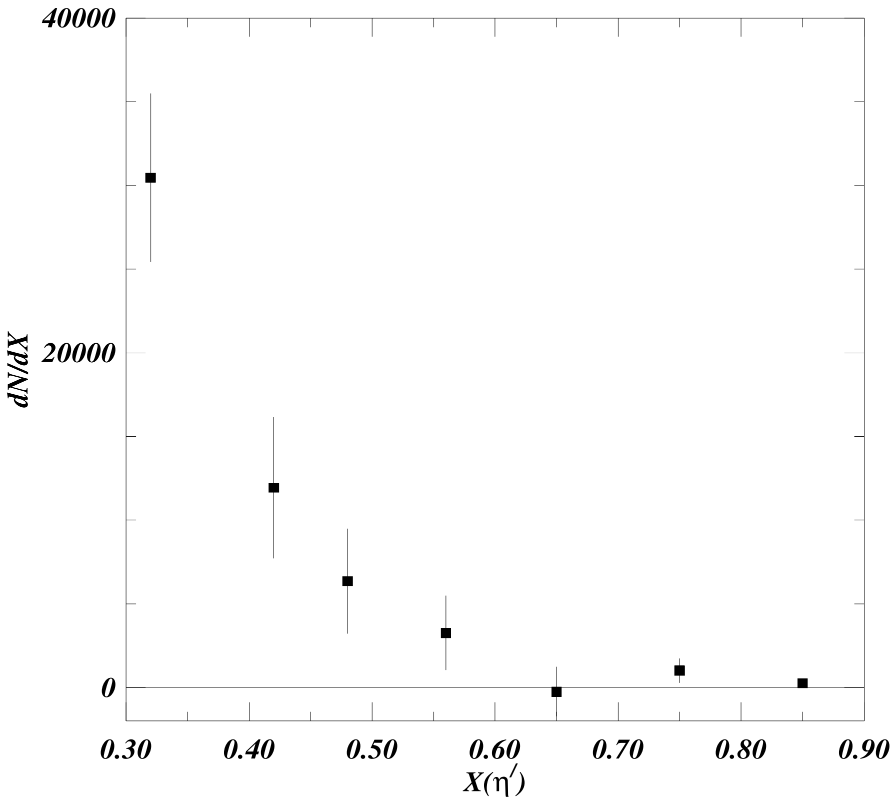


FIG. 9. The continuum-subtracted, efficiency-corrected $dN(B \to \eta^{'})/dx$ as a function of $x$ for $x > 0.30$. The region $0.39 < x < 0.52$ is the $b \to s\ g$ signal region.

## IV. SEARCH FOR HIGH MOMENTUM $\eta^{'}$ AND $K_S$ MESONS.

### A. High momentum $\eta^{'}$ production from $b \to s\ g$

We now the examine the high momentum region. The signal region for $\eta^{'}$ production from $b \to s\ g$ is the momentum bins with $0.39 < x < 0.52$. This region can be further subdvided into two parts: $0.39 < x < 0.45$ and $0.45 < x < 0.52$. In the lower momentum portion, there may be contributions from both $b \to s\ g$ decays and $B \to D^{(*)0}\eta^{'}$ while in the higher x portion, only $b \to s\ g$ contributes.

The upper limits on the number of events in the $b \to s\ g$ search are determined by integrating the likelihood function in the physically allowed region i.e. from 0 to $N_{max}$ so that the area in this interval is 0.90 times the area in the physically allowed region. This is the prescription of the Particle Data Group. Other prescriptions will give slightly different upper limits.

The yields for this region are summarized in Table II. The yield is plotted as a function of $x$ in Fig. 9. From Table II, one has $N_{excess} = 85 \pm 42$ events in the bin with $0.45 < x < 0.52$. This corresponds to an upper limit of $N_{excess} < 131$ events at the 90% confidence level. For the region $0.39 < x < 0.52$, we find an excess of $N_{\eta^{'}} = 222 \pm 66$ events or $N_{\eta^{'}} < 305$. This corresponds to a branching fraction of $Br(B \to \eta^{'} X) = (1.01 \pm 0.30(stat) \pm 0.18(sys)) \times 10^{-3}$ or

$$\mathcal{B}(B \to \eta^{'} X) < 1.70 \times 10^{-3}$$

for $0.39 < X_{\eta^{'}} < 0.52$. In addition, we find no significant excess or deficit in the control region.

In addition to internal spectator decays, other background sources in the high momentum region include $B \to D^{(*)}\pi\eta^{'}$ where the $\eta^{'}$ comes from quark popping at the lower part of the Feynman diagram. We can estimate the contribution of this background from the CLEO measurement of $\mathcal{B}(B \to \pi\pi D)$. Assuming that $B \to D^{(*)}\pi\eta^{'}$ is comparable to non-resonant $B \to \pi\pi D$ and noting that only 6.3% of these $\eta^{'}$s lie in the high momentum search region, we find that the effective branching fraction of this background is $\mathcal{B}(B \to \pi\eta^{'} D) \sim 0.8 \times 10^{-4}$.

In addition, two-body decay modes such as $B \to D\pi^-, D\rho^-, D_s^+\pi^-, D_s^+\rho^-$ with $D \to \eta^{'}\pi/K, D_s^+ \to \eta^{'}\pi^+/\rho^+$ may contribute. In these decays, the $D$ decay must be asymmetric in order to give an $\eta^{'}$ in the momentum interval. The background from these sources is estimated to have an effective branching fraction of $< 0.35 \times 10^{-4}$.

As shown in Table III the detection efficiency for the inclusive analysis is nearly independent of decay mode (e.g. $B \to K^{(*)}\eta^{'}$, $B \to K(1780)\eta^{'}$ ..), provided the decay mode produces $\eta^{'}$ mesons in the range $2.0 - 2.7$ GeV.

### B. High momentum $K_s$ production from $b \to s\ g$

Candidate $K_s$ mesons were selected from pairs of oppositely charged tracks which pass the standard track quality requirements. We impose momentum-dependent requirements on the impact parameter of each track used in the $K_s$ and require that the distance between the center of beam and $K_s$ vertex be greater than 5 mm.

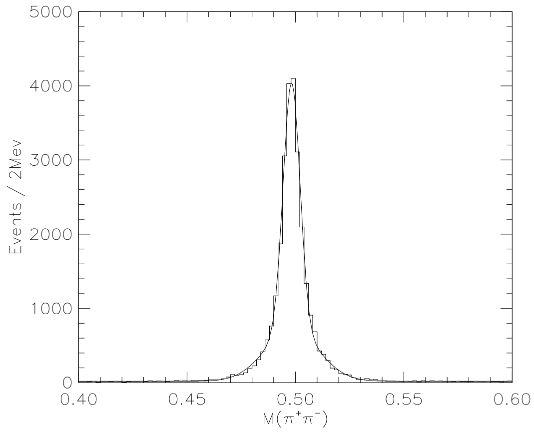


FIG. 10. The $\pi^+\pi^-$ invariant mass for (a) on-resonance data and (b) below resonance data with $0.40 < x < 0.54$.

In each $x$ bin, we fit the continuum subtracted $\pi^+\pi^-$ invariant mass spectrum to the sum of two gaussians and a 1st order Chebyshev function. Two approaches to fitting the data have been tried. It is possible either to fit the $\pi^+\pi^-$ invariant mass plots in the on-resonance and off-resonance samples separately and then subtract the resulting yields, or to fit the continuum-subtracted $\pi^+\pi^-$ invariant mass plots. The latter is chosen for the final result. The difference between the first and second method is used to estimate the systematic error. An example of the raw $\pi^+\pi^-$ invariant mass distributions is shown is Fig. 10. The parameters of the $K_s$ signal are constrained to be the same for on-resonance and continuum data. The results of the fits to the continuum-subtracted distributions are shown in Figs. 11 and 12.

After properly accounting for the energy dependence of the cross section, the continuum subtraction may be slightly biased. This effect is due to the additional energy dependence of the event shape. As the center of mass energy increases, the event shape becomes jettier so that the efficiency of a given cut may change slightly. This bias has been previously investigated in CLEO's inclusive $b \to s\gamma$ analyses. In this analysis, the continuum oversubtraction was determined by parametric Monte Carlo simulation. and found to be a 0.7% effect. In the case of an inclusive analysis with a small continuum subtraction, this bias can be neglected. For example, it is a small effect in the $B \to \eta^{'}$ analysis. The size of this correction (denoted $\delta$) is shown in Table IV. The yield adjusted for the oversubtraction is denoted $N_{sub}^{'}$. The corresponding upper limit is $N_{ul}^{'}$.

The signal region is the scaled momentum bin $0.4 < x < 0.54$. After correcting for the detection efficiency, the continuum oversubtraction, the systematic error (18%), and the $K_s \to \pi^+\pi^-$ branching fraction, we divide by the number of produced B mesons and obtain a 90% confidence level upper limit of

$$\mathcal{B}(B \to K_s X) < 7.5 \times 10^{-4}$$

for $0.40 < x < 0.54$. The upper limits on the branching fractions for $K_s$ production in

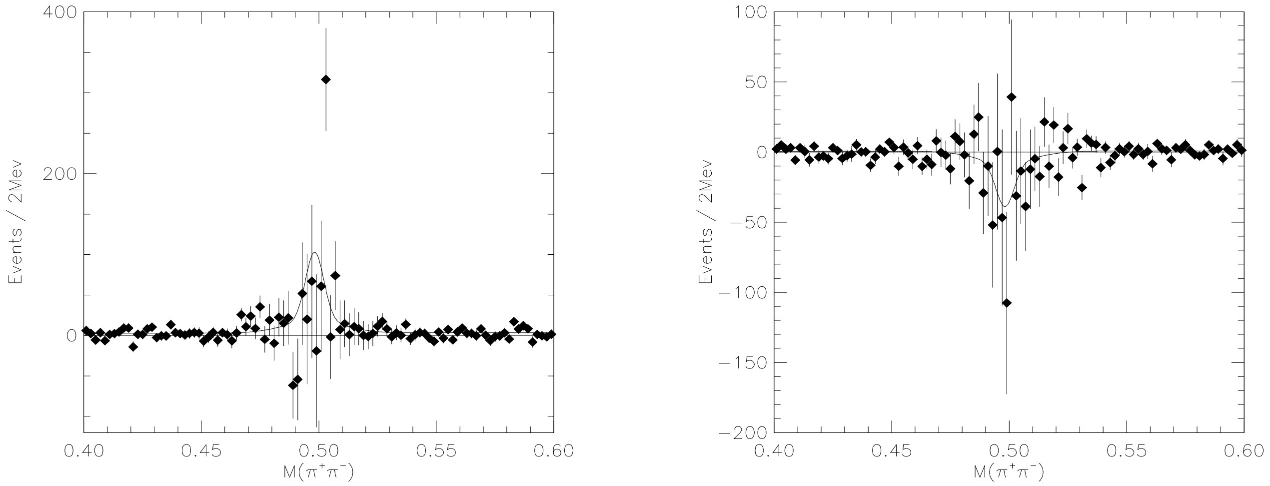


FIG. 11. The $\pi^+\pi^-$ invariant mass distributions for (a) $0.40 < x < 0.45$ and (b) $0.45 < x < 0.54$

the high momentum region are given in Table V. As with the $\eta^{'}$ analysis, the continuum-suppression cuts have been loosened for the control bins. We find no significant excess or deficit in the control region (see Fig. 13).

We now discuss the components of the systematic uncertainty for the endpoint region of $B \to K_s$. The uncertainty in the background shape is determined by comparing the result of separate fits to the on-resonance and continuum yields with fits to the plots which were continuum subtracted. We also compare fits with different background parameterizations. The error due to the signal shape is found by varying the signal parameters within their errors. The largest component of the systematic error is the uncertainty in the continuum oversubtraction, 0.35%, which gives a systematic uncertainty of $\pm 10\%$. As was the case for high momentum $B \to \eta^{'}$, the detection efficiency is not sensitive to the decay mode considered (see Table VII).

## V. CONCLUSIONS

We have measured $\dfrac{d\mathcal{B}(B \to \eta^{'} X)}{dx}$ and determined

$$\mathcal{B}(B \to \eta^{'} X) = (3.06 \pm 0.61(stat) \pm 0.55(sys)) \times 10^{-2}$$

for the range $0.10 < x_{\eta^{'}} < 0.39$ where $b \to c$ processes dominate. The observed momentum spectrum of $\eta^{'}$ is in agreement with the CLEO Monte Carlo model of $B$ decay.

There is a modest excess observed in the signal region for quasi two-body $B \to \eta^{'} X_s$ decays. In addition, there is no significant excess or deficit in the control region. We find a 90% confidence level upper limit of

$$\mathcal{B}(B \to \eta^{'} X_s) < 7.4 \times 10^{-4}$$

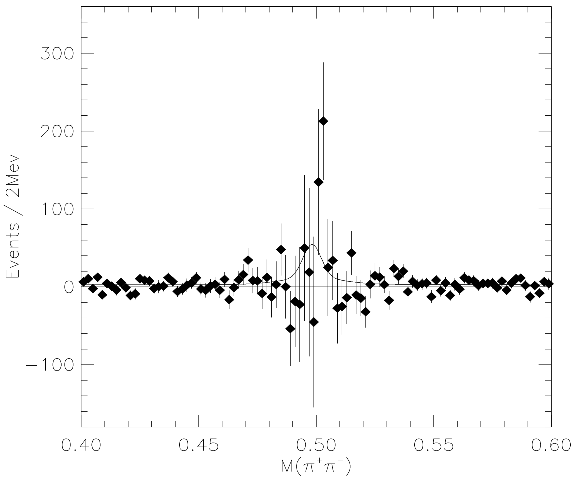


FIG. 12. The $\pi^+\pi^-$ invariant mass distributions for $0.40 < x < 0.54$

for the range $0.45 < x_{\eta'} < 0.52$. We also obtain an upper limit for the larger momentum interval $0.39 < x_{\eta'} < 0.52$, where both $b \to s\, g$ and internal spectator decays may contribute, of

$$\mathcal{B}(B \to \eta' X_s) < 1.7 \times 10^{-3}.$$

Examination of high momentum $K_s$ production gives a 90% confidence level upper limit of

$$\mathcal{B}(B \to K_s X) < 7.5 \times 10^{-4}$$

for $0.4 < x_{K_s} < 0.54$. In the range $0.46 < x < 0.54$ where only $b \to s\bar{d}d$ transitions may contribute, we obtain the upper limit

$$\mathcal{B}(B \to K_s X) < 2.1 \times 10^{-4}.$$

It is not clear how the $X_{(s)}$ system will hadronize, and in what momentum range the $K_s$ and $\eta'$ mesons from $b \to s\, g$ will be produced. It is conceivable that the hadronization of the $X_s$ system will be very different from the case of $b \to s\gamma$ [7], [8]. In particular, Milana and Nussinov suggest that $B \to K_s X$ from $b \to s\, g$ will not be dominated by a few resonances [7].

The inclusive analysis described in this note gives a limit for $0.4 < x_{meson} < 0.54$ which is nearly *independent* of the hadronization scheme. In the near future, we will apply the $B$ reconstruction method which was previously used for CLEO's measurement of $b \to s\gamma$ and the $B \to X_s\phi$ search to the $B \to K_s$ and $B \to \eta'$ channels. This method will provide better discrimination against continuum backgrounds.

The conversion of the upper limits on $\mathcal{B}(B \to K_s X)$, $\mathcal{B}(B \to \eta' X)$, to upper limits on $\mathcal{B}(b \to s \text{ gluon})$ is also theoretically quite uncertain. Thus, at present, it is not yet possible to rule out certain proposed extensions of the Standard Model involving either supersymmetry or technicolor. For example, Hou [9], A. Kagan [10], Ciuchini et. al. [5], and others have

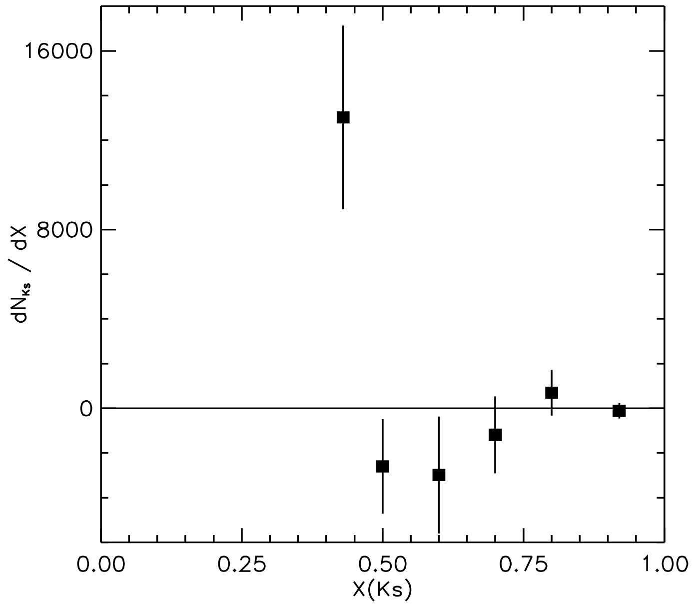


FIG. 13. The yield of $K_s$ as a function of $x$ (scaled momentum).

proposed $\mathcal{B}(b \to s\ gluon) \sim 10\%$ or $\mathcal{B}(b \to d\ gluon) \sim 10\%$ [10], rather than $\mathcal{O}(1\%)$ as is expected in the Standard Model, in order to explain the $B$ semileptonic branching fraction problem and the apparent low charm quark yield in $B$ decay. These models do not necessarily modify $\mathcal{B}(b \to s\gamma)$.

## ACKNOWLEDGEMENTS

We gratefully acknowledge the effort of the CESR staff in providing us with excellent luminosity and running conditions. J.P.A., J.R.P., and I.P.J.S. thank the NYI program of the NSF, M.S thanks the PFF program of the NSF, G.E. thanks the Heisenberg Foundation, K.K.G., M.S., H.N.N., T.S., and H.Y. thank the OJI program of DOE, J.R.P, K.H., and M.S. thank the A.P. Sloan Foundation, and A.W., and R.W. thank the Alexander von Humboldt Stiftung for support. This work was supported by the National Science Foundation, the U.S. Department of Energy, and the Natural Sciences and Engineering Research Council of Canada.

## TABLES

TABLE I. Systematic errors in the measurement of the $B \to \eta^{'}$ branching fraction.

| Source | $\Delta(\mathcal{B}(B \to \eta^{'}))$ |
|---|---|
| continuum subtraction | $\pm 0.05\%$ |
| background shape | $\pm 15\%$ |
| parameters of signal | $\pm 1.2\%$ |
| continuum oversubtraction | $\pm 0.8\%$ |
| photon detection efficiency | $\pm 5\%$ |
| track detection efficiency | $\pm 4\%$ |
| total | $\pm 17.6\%$ |

TABLE II. Summary of $\eta^{'}$ yields in the purely inclusive analysis

| $X_{\eta'}$ | On 4S | Below 4S | Subtracted | Yield |
|---|---|---|---|---|
| 0.10-0.20 | 1519±162.5 | 246.9±59.1 | 1052±198 | 26974±5071 |
| 0.20-0.28 | 1125±155 | 157±51 | 825±180 | 5322±1162 |
| 0.28-0.39 | 1281±88 | 311±38 | 687±113 | 3351± 554 |
| 0.39-0.45 | 380±34 | 126±19 | 139±50 | 716±253 |
| 0.45-0.52 | 320±27 | 123±17 | 85±42 | 445±220 |
| 0.52-0.60 | 375±26 | 164±17 | 62±42 | 261±178 |
| 0.60-0.70 | 202±19 | 109±15 | -6±35 | -25±148 |
| 0.70-0.80 | 93±11 | 36±7 | 24±17 | 101±72 |
| 0.80-1.00 | 26± 5 | 7±3 | 12±8 | 51±134 |

TABLE III. Detection efficiency for various decay modes in the inclusive $\eta'$ analysis.

| Mode | $\epsilon$ |
|---|---|
| $B \to K^*(892)\eta'$ | $16.8 \pm 1.3\%$ |
| $B \to K_1(1270)\eta'$ | $17.6 \pm 1.1\%$ |
| $B \to K_0^*(1430)\eta'$ | $19.6 \pm 1.2\%$ |
| $B \to K_1^*(1460)\eta'$ | $17.4 \pm 1.1\%$ |
| $B \to K_2^*(1430)\eta'$ | $17.0 \pm 1.1\%$ |
| $B \to K_3^*(1780)\eta'$ | $18.9 \pm 1.3\%$ |

TABLE IV. $B \to K_s X$ yield as a function of $x$

| $x_{K_s}$ | $N_{sub}$ | $N_{ul}$ | $\delta(\%)$ | $N'_{sub}$ | $N'_{ul}$ |
|---|---|---|---|---|---|
| 0.40-0.46 | 648±240 | 895 | -0.70±0.14 | $781 \pm 241$ | 1063 |
| 0.46-0.54 | -277±169 | 145 | -0.70±0.14 | $-209 \pm 169$ | 231 |
| 0.40-0.54 | 344±282 | 645 | -0.70±0.14 | $530 \pm 284$ | 879 |
| 0.54-0.65 | -234±287 | | 0.35±0.09 | $-329 \pm 288$ | |
| 0.65-0.75 | -85±172 | | 0.35±0.09 | $-119 \pm 173$ | |
| 0.75-0.85 | 88±102 | | 0.54±0.37 | $70 \pm 103$ | |
| 0.85-1.00 | -13±52 | | 0.54±0.37 | $-17 \pm 52$ | |

TABLE V. Branching Fraction Upper Limits for $B \to K_s X$ $(\times 10^{-4})$

| $x_{K_s}$ | $N'_{sub}$ | $\varepsilon$ | $\mathcal{B}(B \to K_s X)$ | $BR'$ | UL BR(with sys) |
|---|---|---|---|---|---|
| 0.40-0.46 | $781 \pm 241$ | 0.364±0.011 | $4.7 \pm 1.5$ | 6.4 | 7.8 |
| 0.46-0.54 | $-209 \pm 169$ | 0.294±0.006 | $-1.6 \pm 1.3$ | 1.7 | 2.1 |
| 0.40-0.54 | $530 \pm 284$ | 0.315±0.005 | $3.7 \pm 2.0$ | 6.1 | 7.5 |

TABLE VI. Systematic errors in the determination of the upper limit $B \to K_s X$ branching fraction.

| Source | $\Delta(\mathcal{B}(B \to K_s))$ |
|---|---|
| continuum subtraction | 15.1% |
| background shape | 5.0% |
| parameters of signal | 0.3% |
| track detection efficiency | 4% |
| $K_s$ detection efficiency | 5% |
| total | 18.3% |

TABLE VII. Detection efficiency for decay modes and hadronization models.

| Mode | $\epsilon$ |
|---|---|
| $B \to K_s\pi$ | $36.6 \pm 1.4\%$ |
| $B \to K_s\rho$ | $33.4 \pm 1.3\%$ |
| $B \to K_s\phi$ | $35.7 \pm 1.4\%$ |
| $B \to K_s a_1$ | $27.6 \pm 1.2\%$ |
| $B \to K_s b_1$ | $29.4 \pm 1.2\%$ |
| $B \to K_s\rho^{'}$ | $27.0 \pm 1.1\%$ |
| $B \to K_s D$ | $30.0 \pm 0.1\%$ |

# REFERENCES


[1] Y. Kubota et al. (CLEO Collaboration), Phys. Rev. D. **53**, 6033, 1996.

[2] R. Grigjanis, P.J. O'Donnell, M. Sutherland, and H. Navelet, Phys. Lett. B. 224, 209 (1989).

[3] N. G. Deshpande, X.-G. He and J. Trampetic, Phys. Lett. B. 377, 161 (1996)..

[4] N. G. Deshpande, G. Eilam, X.-G. He and J. Trampetic, Phys. Lett. B. 366, 300 (1996)..

[5] M. Ciuchini, E. Gabrielli, and G.F. Guidice, CERN-TH-96-073, hep-ph/9604438 and private communication.

[6] K. W. Edwards et al. (CLEO Collaboration), (CLEO CONF 95-8).

[7] J. Milana and S. Nussinov, Phys. Rev. D. **51**, 1192, (1995).

[8] J. Swain, preprint NUB-3101 and hep-ph/9501415.

[9] B. Grzadkowski, W.-S. Hou, Phys. Lett. B. **272**, 383, (1991).

[10] A. L. Kagan, Phys. Rev. D. 61, 5196 (1995) and hep-ph/9409215.